

# Monitoring seaweed aquaculture in the Yellow Sea with multiple sensors for managing the disaster of macroalgal blooms

Qianguo Xing<sup>a,b,c,\*</sup>, Deyu An<sup>a,b,c</sup>, Xiangyang Zheng<sup>a,b,c</sup>, Zhenning Wei<sup>a,b,c</sup>, Xinhua Wang<sup>a,b,c</sup>, Lin Li<sup>a,b,c</sup>, Liqiao Tian<sup>d</sup>, Jun Chen<sup>e</sup>

<sup>a</sup> CAS Key Laboratory of Coastal Environmental Processes and Ecological Remediation, Yantai Institute of Coastal Zone Research, Chinese Academy of Sciences, Yantai, China

<sup>b</sup> Center for Ocean Mega-Science, Chinese Academy of Sciences, Qingdao, China

<sup>c</sup> University of Chinese Academy of Sciences, Beijing, China

<sup>d</sup> Wuhan University, Wuhan, China

<sup>e</sup> Xi'an Jiaotong University, Xi'an, China

## ARTICLE INFO

Edited by Emilio Chuvieco

### Keywords:

Multi-sensor observation  
Marine hazard  
Floating algae  
Human activity  
Seaweed cultivation  
The Yellow Sea

## ABSTRACT

Multi-sensor remote sensing is a critical part of the surveillance of coastal ocean for hazard management. The world's largest green macroalgae blooms (green tide) in the Yellow Sea since 2007 are caused by the macroalgae of *Ulva*, which are disposed as biofouling into sea water when workers recycle seaweed (*Porphyra*) farming facilities. We traced the development processes of seaweed cultivation in which area since 2000 and the variation in macroalgal blooms since 2007 through multi-sensors (satellite, Unmanned Aerial Vehicle, and ground spectroradiometer) remote sensing in this study. We found that the sudden occurrence of large-scale green tide in 2007 and the increasing trend since that year were caused by the seaweed aquaculture in a specific mode at specific locations. A numerical simulation and satellite observations on the relationship between the timing of recycling seaweed facilities and the volume of green tide suggest that the green tide is manageable. Adoption of multi-sensor, multi-scale, and multi-temporal observations, translocating seaweed farming sites, and changing the cultivation mode are deemed as key tools for controlling the green tide and sustaining the seaweed aquaculture.

## 1. Introduction

Due to intensifying human activities and climate change, sustainable development of coastal zones has been threatened by various anthropogenic and natural disasters. The world's largest green tide caused by the green macroalgae blooms (MABs) of *Ulva prolifera* has occurred in the Yellow Sea every summer since 2007 (Hu and He, 2008; Xing et al., 2018), bringing not only huge economic loss (Wang et al., 2009) but also wide-spread ecological and environmental impacts, e.g., on phytoplankton biomass, water clarity in ten thousand square kilometers (Xing et al., 2015a; Li et al., 2018) and zooplankton community in coastal waters (Wang et al., 2019).

Different from green tides in other coastal waters (Lapointe et al., 2004; Bohórquez et al., 2013), the floating *U. prolifera* in the Yellow Sea were reported to be originated from the *Porphyra yezoensis* cultivation region (Liu et al., 2009; Keesing et al., 2011; Wang et al., 2015; Xing et al., 2018). After the *P. yezoensis* harvesting in every April, workers

start to recycle the facilities, i.e., the nets, ropes and poles for re-use in the next cultivation cycle. During the facility recycling, green macroalgae of *U. prolifera* attached to the *P. yezoensis* cultivation facilities are scraped as biofouling and discarded into sea water; the discarded macroalgae grow rapidly under favorable light, temperature and nutrient conditions (Liu et al., 2009; Zhou et al., 2015; Jin et al., 2018), and form large-scale green tide in June and July. Satellite observations (Xing et al., 2011, 2015b, 2018; Qi et al., 2016; Hu et al., 2017, 2019) documented the seasonal pattern of the green tide, i.e., the initial appearance of green tide in the Jiangsu Shoal waters in late April and early May, the peak in late June in the offshore waters of the western Yellow Sea, and the disappearance in the coastal waters of the Shandong Peninsula in late July and August.

The MABs in the Yellow Sea can be dated back to 1999 (Hu et al., 2010; Xing and Hu, 2016), which is in agreement with the four decades of *P. yezoensis* cultivation history in the coastal waters of the western Yellow Sea. The progressive eutrophication of sea water in the Yellow

\* Corresponding author at: Yantai Institute of Coastal Zone Research, Chinese Academy of Sciences, Yantai, China.

E-mail address: [qgxing@yia.c.cn](mailto:qgxing@yia.c.cn) (Q. Xing).

<https://doi.org/10.1016/j.rse.2019.111279>

Received 5 October 2018; Received in revised form 17 June 2019; Accepted 22 June 2019

Available online 28 June 2019

0034-4257/ © 2019 The Author(s). Published by Elsevier Inc. This is an open access article under the CC BY-NC-ND license

(<http://creativecommons.org/licenses/by-nc-nd/4.0/>).

Sea (Xing et al., 2015b) and the gradual expansion of *P. yezoensis* cultivation area in the entire Jiangsu Shoal (Wei et al., 2018) might not have led to the sudden occurrence of large-scale MABs in this region in 2007 and 2008. Studies showed how local wind and currents impacted the drifting path of green tide (Xing et al., 2009; Lee et al., 2011; Qiao et al., 2011; Zheng et al., 2011; Bao et al., 2015; Xu et al., 2016), and indicated roughly the origin being the Jiangsu Shoal *P. yezoensis* cultivation region (Son et al., 2015; Zhang et al., 2017). However, detailed spatio-temporal evolution of *P. yezoensis* cultivation and how it impacts the green tide are not known. Answers to these questions are critical for the management of *P. yezoensis* seaweed cultivation and the counter-measures responding to the green tide.

In this study, multi-sensor remote sensing data from satellite and in-situ observations are used to retrieve the multi-temporal and multi-spatial evolution in the *P. yezoensis* cultivation in the southern Yellow Sea, and numerical simulation is used to determine the contribution of the green macroalgae released from different seaweed farming zones. Through examining the impacts of seaweed aquaculture development and activities on the green tide, we intend to offer solutions to control the green tide while sustaining the seaweed aquaculture.

## 2. Data and methods

### 2.1. Multi-sensor, multi-temporal and multi-spatial remote sensing

As shown in Fig. 1, various cruises have been carried out in China's

coastal waters for field observations. However, the information collected during these cruises is very limited in terms of spatial and temporal coverage. Historical data of marine culture can be retrieved from China Fisheries Statistical Yearbook as in Xing et al. (2015b); however, they are also limited by accuracy and by spatial and temporal resolution. Traditional data are not adequate to support an effective surveillance of massive aquaculture along China's coast and the management of widespread marine disaster of algal blooms.

Due to complex environmental conditions, an integration of satellite and in-situ data is necessary for the assessment of coastal oceans by remote sensing techniques (Warren et al., 2015; Xing et al., 2018). To improve the efficiency of such integration, a strategy of multi-sensor, multi-temporal and multi-spatial (3M) remote sensing is employed in the surveillance of coastal aquaculture and monitoring macroalgal blooms. As shown in Fig. 1, this includes satellite observations, Unmanned Aerial Vehicle (UAV) and field measurements. Different sensors provide different data at multi-temporal and multi-spatial scales, which are integrated and used for different purposes (see Table 1).

### 2.2. Seaweed farming modes of *P. yezoensis*

This study focuses on the *P. yezoensis* farming regions along the western coast of the southern Yellow Sea (Fig. 2a), which is suspected to be the source of *U. prolifera* green tide (Liu et al., 2009). There are two major farming regions of *P. yezoensis* (Xing et al., 2015b; Wei et al., 2018): one is featured by the offshore waters away from the low tide

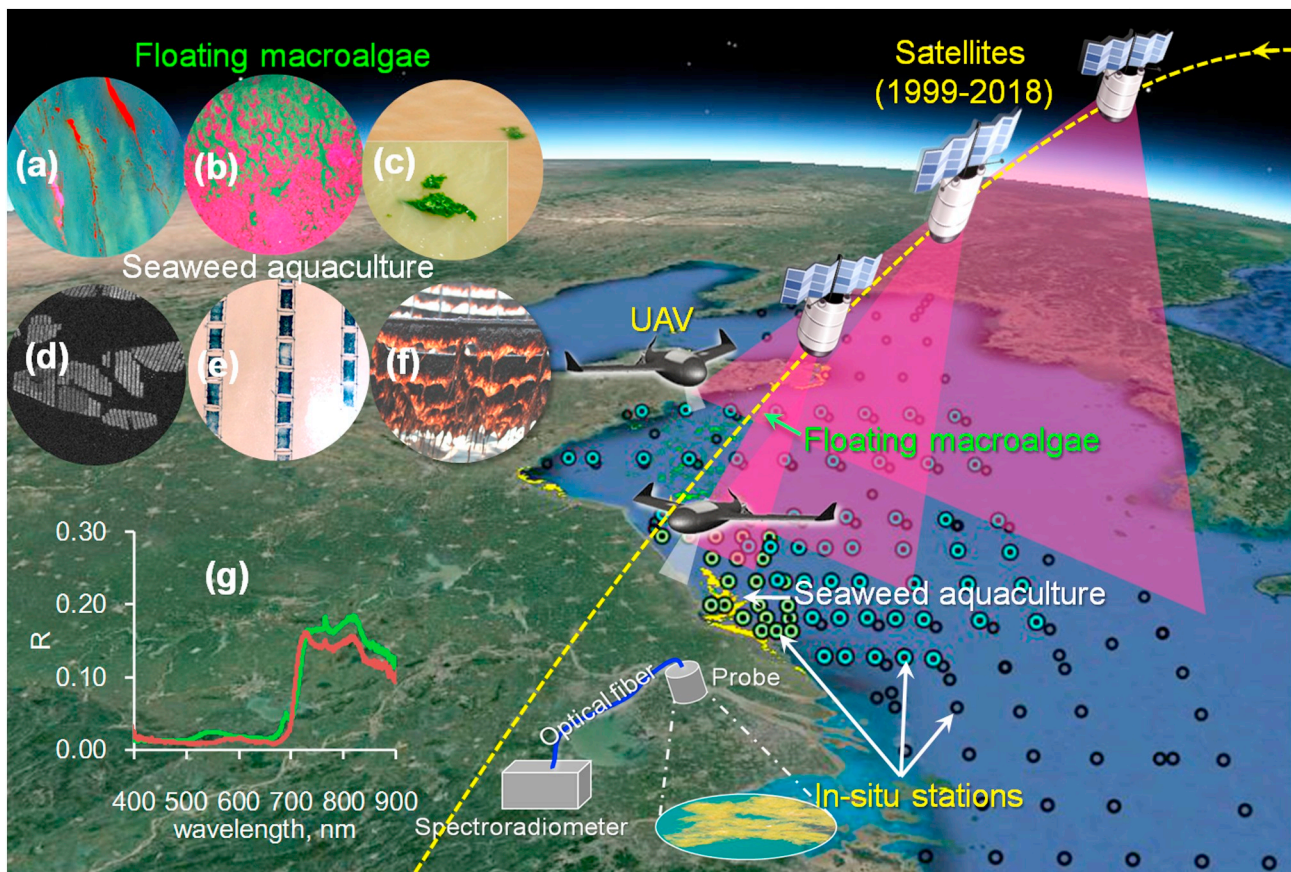


**Fig. 1.** Schematic of multi-sensor, multi-temporal and multi-spatial (3M) remote sensing for the surveillance of macroalgal blooms and seaweed aquaculture in China. The insets (a), (b) and (c) are floating macroalgae in satellite image (composite of GaoFen-1 NIR-red-green bands), UAV image (false colour composite of NIR-red-green bands), and in-situ photos, respectively; (d), (e) and (f) are seaweed aquaculture in satellite image (Sentinel-1A VH polarization), UAV true colour image, and in-situ photo, respectively. (g) shows reflectance collected by ground spectroradiometer in field work: the green curve is for the green macroalgae of *U. prolifera*, and the brown curve is for the seaweed of *P. yezoensis*. The symbols of ○, ◻ and ◻ show the stations during the cruises in the Yellow Sea and East China Sea, the western South Yellow Sea and the Jiangsu Shoal, respectively (Xing et al., 2015b; Zhang et al., 2015b). (For interpretation of the references to colour in this figure legend, the reader is referred to the web version of this article.)

**Table 1**

Multi-sensor, multi-scale and multi-temporal data and their uses in monitoring seaweed farming and floating macroalgal blooms.

Sensors		Resolution	Revisit	Starting year in use and use description
Satellites (optical)	Landsat TM/ETM+/OLI	30 m	15 days	1999, to extract seaweed farming region
	GaoFen-1 WVF	16 m	4 days	2016, to extract the seaweed farming region and the early macroalgal blooms
	Sentinel-2 A/B	10 m	10 days	2016, to extract the seaweed farming region
	MODIS terra/aqua	250 m	One day	2000, to extract the annual maximum daily macroalgal blooms
Satellites (Microwave)	Sentinel-1A/B	5 * 5 m	12 days	2016, to extract seaweed farming region on tidal flat for cross-sensor validation
UAV	DJI R-G-B/NIR-R-G	< 25 cm	-	2016, to collect in-situ multi-spectral images for validating the satellite-derived results
Spectro-radiometer	OOI SD2000/USB4000	-	-	2008, to collect reflectance (400–900 nm) in field work for algorithm testing

waterline near the city Lianyungang in the northern Jiangsu Province, and the other is featured by the intertidal zones of the Jiangsu Shoal. Accordingly, there are two different modes of *P. yezoensis* cultivation.

- (1) Mode-I in the Lianyungang cultivation region (Fig. 2b): Poles are inserted into the seabed, and the height of nets can be adjusted to ensure enough exposure time to air and sunlight for the growth of *P. yezoensis*.
- (2) Mode-II in the Jiangsu Shoal cultivation region (Fig. 2c): The height of nets is fixed, and thus the net-exposure duration is regulated by the tidal cycle. The *P. yezoensis* cultivation in the Jiangsu coastal

waters usually starts from autumn to the next spring, and the winter season (December, January and February) is the best for the growth of *P. yezoensis*.

### 2.3. Extraction of *P. yezoensis* farming regions

The cultured *P. yezoensis* is brown (Fig. 1f), which has strong absorption in the red band and shows the red edge in the visible and near-infrared reflectance spectra as the floating brown macroalgae of *Sargassum* (shown in Fig. 1g; Xing et al., 2017; Li et al., 2018). Thus, the *P. yezoensis* nets (Fig. 2c) may be detected on the basis of spectral feature.

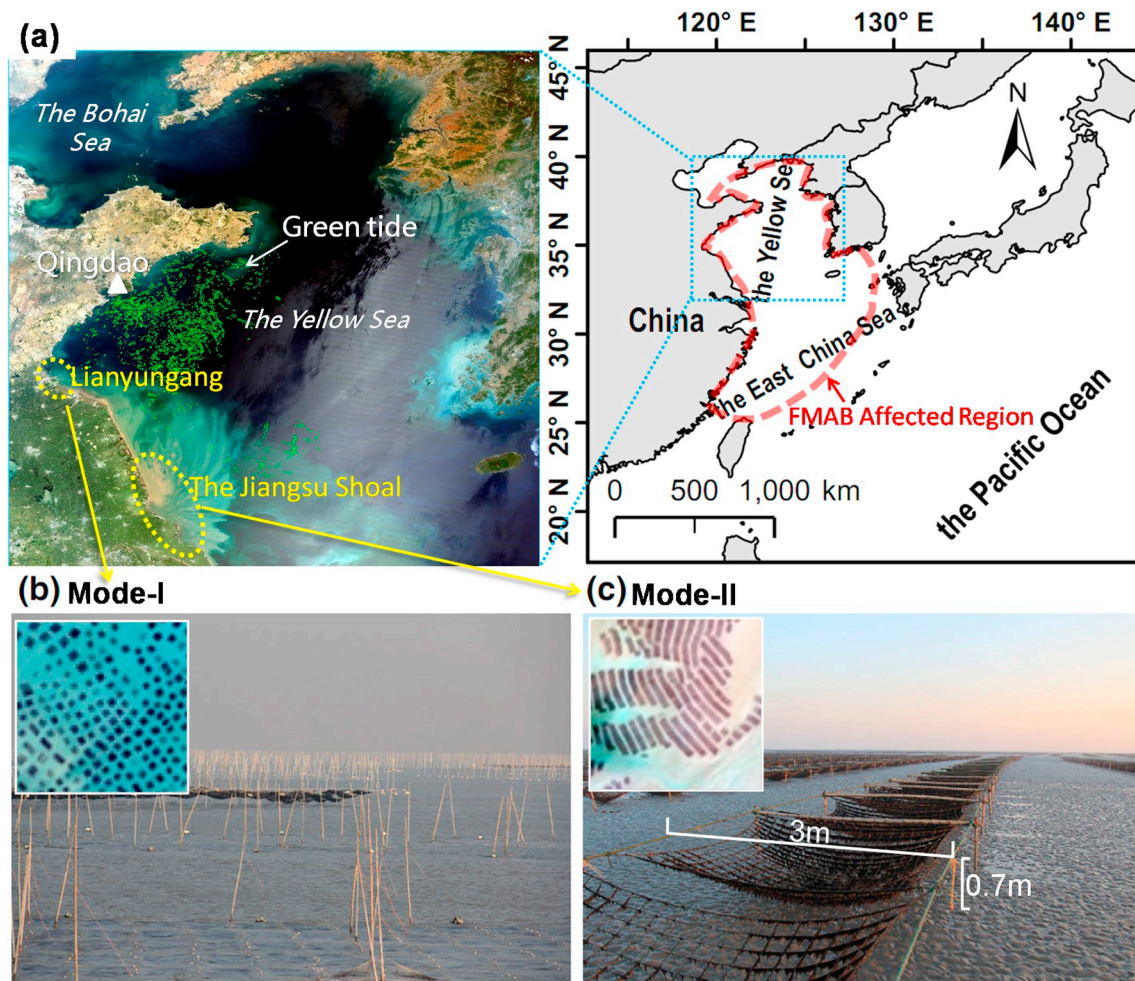


**Fig. 2.** (a) Map of the study area. The true colour image is a composite of Moderate Resolution Imaging Spectrometer (MODIS) band #1 (Red), band #4 (Green) and band 3 (Blue) acquired on 6 May 2009, in which the green slicks show the green tide in 2008 and 2009. The dashed red line shows the region visited by floating macroalgal blooms (FMAB) in the Yellow Sea and East China Sea based on satellite observation results. This figure uses unpublished data and the data from several published studies (Xing et al., 2011, 2015b; Xing and Hu, 2016). (b) and (c) show in-situ photos of *P. yezoensis* farming in a height-adjustable mode in the deep water near Lianyungang (Mode-I), and a height-fixed mode on the tidal flats of the Jiangsu Shoal (Mode-II), respectively (after Xing et al., 2015b); the insets are the corresponding Landsat images of the *P. yezoensis* cultivation, respectively. (For interpretation of the references to colour in this figure legend, the reader is referred to the web version of this article.)

Specifically, the red band (Red) and near-infrared band (NIR) data acquired by optical satellite sensors are processed to give top-of-the-atmosphere reflectance (R, unitless). Then, the difference vegetation index (DVI), i.e., the reflectance difference between the NIR band and the Red band ( $R_{NIR} - R_{Red}$ ), which has a linear correlation to the coverage of macroalgae (Xing et al., 2018), is calculated for each image.

For the farming region of mode-I where there is no impact from the tidal flat, the DVI is used to extract the *P. yezoensis* cultivation area (PCA, km<sup>2</sup>). For mode-II in the tidal flat where the *P. yezoensis* farming zone usually shows belt-shaped features in satellite images, the farming zone is outlined on the basis of visual inspection and the DVI index (Wei et al., 2018). Micro-wave data used to detect floating macroalgae (Shen et al., 2014) is also used to verify the detection of the *P. yezoensis* facilities on the tidal flat. As shown in Figs. 1d, 2b and c, the *P. yezoensis* farming regions have higher backscattering than the background of water or tidal flat in the Sentinel-1A micro-wave image.

To reduce the impacts from clouds and tidal level changes, 3–5 images acquired in winter and early spring are used to extract the PCA in every *P. yezoensis* cultivation cycle; then, the results extracted from temporally different images are used to compose the maximum PCA. According to data availability and spatial resolution, Landsat images are used to retrieve the annual PCA in Lianyungang (mode-I) as well as the Jiangsu Shoal (mode-II) during the period of 2000–2018.

High-resolution GaoFen-1, Sentinel-2 and Landsat-8 images are used to monitor the dynamics in the *P. yezoensis* facilities recycling during the period from the end of April to early June of 2016–2018. The spatial resolutions of Sentinel-2, GaoFen-1 and Landsat images used for monitoring the *P. yezoensis* farming regions are 10, 16 and 30 m, respectively. The width of *P. yezoensis* farming nets is usually about 3 m (as shown in Fig. 2c), lower than the ground resolutions of GaoFen-1, Sentinel-2 and Landsat-8 images. Thus, pixel-mixing effects may lead to biased results, which are derived on the basis of images with different resolutions. Image pairs over the same *P. yezoensis* farming region with a gap of acquisition dates less than five days are selected to investigate the consistency in the retrieved coverage area of *P. yezoensis* facilities. The areas derived from different image pairs are then compared, and two linear regression functions ( $R^2 > 0.995$ ) between the areas derived from Sentinel-2 and Landsat-8 images and those from GaoFen-1 image are established to convert the results to the level of GaoFen-1 in this work (as shown in Fig. 3).

#### 2.4. Remote sensing of floating *Ulva* macroalgae and biomass prediction

Optical satellite images were proposed to extract floating macroalgae in previous studies (Hu, 2009; Liu et al., 2009; Shi and Wang, 2009; Xing and Hu, 2016). Satellite images over the Yellow Sea acquired in May–July since 2007 were collected, and those with low-

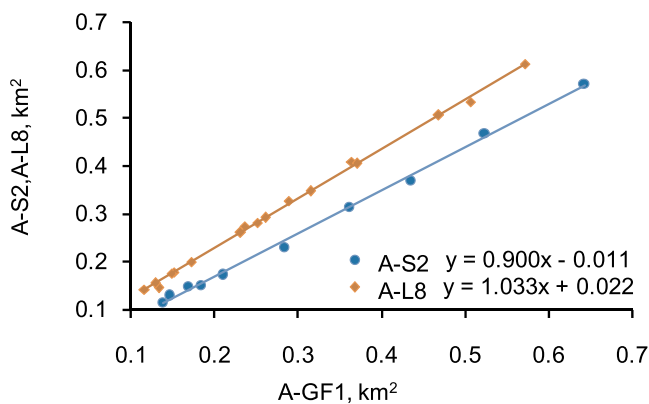


Fig. 3. Comparison in the *P. yezoensis* facility coverage areas derived from the optical images of GaoFen-1, Sentinel-2 and Landsat-8, i.e., A-GF1, A-S2 and A-L8, respectively.

cloud coverage were selected for extracting MABs, including the images of GaoFen-1 and the Moderate Resolution Imaging Spectrometer (MODIS).

Macroalgae have higher reflectance-based DVI values than the background sea water. In this work, dynamic threshold of DVI is used to extract macroalgae pixels: A DVI image is segmented into small windows whose sizes vary with the images with different resolutions (e.g., the sizes range from 30\*30 pixels to 300\*300 pixels for MODIS images, while from 100\*100 pixels to 2000\*2000 pixels for GaoFen-1 images), and a threshold is set to classify macroalgae pixels window by window, i.e., pixels with their DVI values larger than the threshold (from  $-0.02$  to  $0.01$ , varying with water optical conditions) are classified as macroalgae pixels. Meanwhile, the R(NIR band)-G(Red band)-B(Green band) false-colour images are used for visual inspection of each window where macroalgae show red or brown colour in the enhanced false-colour image. The areas of macroalgae pixels extracted in the small windows are then summed to give the total coverage area of MABs (km<sup>2</sup>) for the entire image.

Fig. 4 shows the forming process of green tide caused by the seaweed farming-facility recycling in every April and May. The floating macroalgae patches have smaller sizes at the early stage, and they expand and form massive green tide usually in June and July. Thus, the high-resolution GaoFen-1 images are used to monitor the early-stage MABs, while the 500-m-resolution MODIS images are used to derive the daily MABs in the open waters. Taking into account the beaching of floating macroalgae since late June and different lasting durations of green tides in different years, the maximum daily MABs (MD-MABs) is selected as a proxy of the annual maximum daily biomass of *Ulva* MABs for analyzing inter-annual changes. The results of MD-MABs derived using the DVI approach in this work are highly similar to those derived by other approaches, for example, the Floating Algae Index (FAI) (Qi et al., 2016).

Due to the limitations in the revisit cycle of satellite and cloud conditions, it is not possible to obtain all the results of MABs on the same day in different years. To compare the initial MABs acquired with different dates in different years, a simplified biomass prediction model on the basis of a uniform growth rate is proposed to estimate the MABs on the date when there is no effective result by satellite observation (see Eq. (1)).

$$A1 = A0 * (1 + G)^N, \quad (1)$$

where  $A0$  is the initial macroalgae coverage area (km<sup>2</sup>, a proxy of biomass) retrieved by satellite observation on the day of the year (DOY1), and  $A1$  is the estimated area (km<sup>2</sup>) for the day of DOY2  $N$  days later ( $N = DOY2 - DOY1$ ).  $G$  is the growth rate of floating green macroalgae in the Jiangsu Shoal waters in May, and in this study it is assumed to be an empirical uniform value of 0.2 per day according to in-situ observations (Zhang et al., 2013) and satellite remote sensing (Xing et al., 2018).

#### 2.5. Simulating the drifting paths of early *U. prolifera* macroalgae

To investigate drifting paths of early floating macroalgae from different sites, the Lagrangian particle tracking (LPT) model is used to determine the locations of floating *Ulva* macroalgae in April and May using the climatological surface ocean circulation in the Yellow Sea. In the LPT method, the location of a particle is integrated by solving an ordinary differential equation set (Eq. (2)), with given spatial and temporal surface current velocity field. A coastline boundary is set in the LPT model, and the particles crossing the coastline are marked as inactive and their locations are no longer updated in the following steps, i.e., these macroalgae particles are considered to have beached, and no longer return to the sea water.

$$dx/dt = U(x, t), \quad dy/dt = V(x, t), \quad (2)$$

where  $x$  and  $y$  give the location of the particle, and  $U$  and  $V$  represent

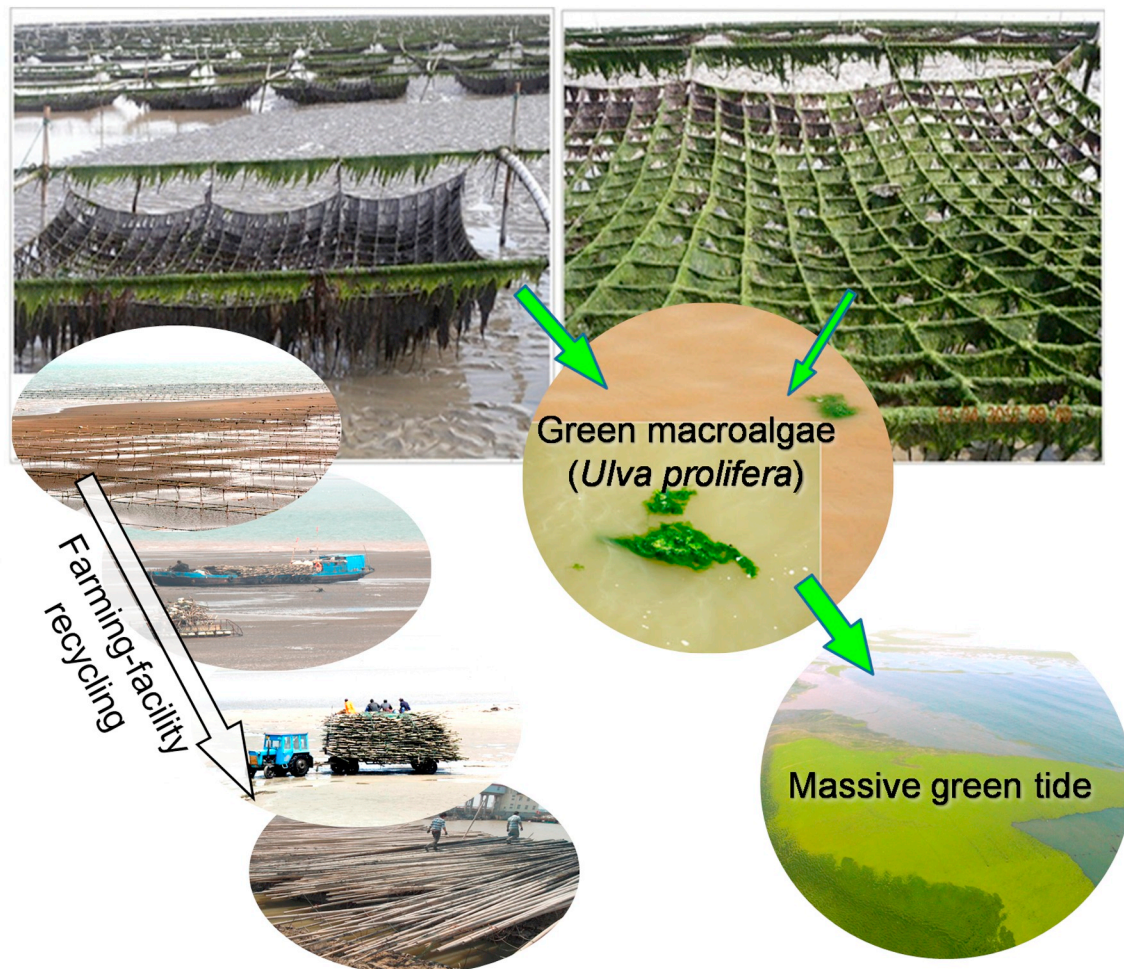


**Fig. 4.** A schematic showing how green tide dominated by *U. prolifera* occurs due to the seaweed farming-facility recycling in April and May. The photos show that the seaweed (*P. yezoensis*) farming facilities are fouled by attached green macroalgae. (For interpretation of the references to colour in this figure legend, the reader is referred to the web version of this article.)

current velocities in x and y directions, respectively.

The surface current velocity data used in this study are monthly averaged, including the effect of wind, tide and density variations. The data are provided by the Marine Science Data Center of the Chinese Academy of Sciences, based on the modeling work of Yang et al. (2018). The spatial resolution of the data is  $0.15^\circ$  in longitude and latitude.

### 3. Results and discussion

#### 3.1. Evolution in *P. yezoensis* cultivation location

As shown by the satellite observation results (Fig. 5), the total PCA in Jiangsu coastal waters increased gradually from  $60 \text{ km}^2$  in 2000 to  $300 \text{ km}^2$  in 2015. In the mode-I cultivation region of Lianyungang (Fig. 5a), the PCA increased from  $10 \text{ km}^2$  in 2000 to  $65 \text{ km}^2$  in 2015. The PCA in the mode-II cultivation region of the Jiangsu Shoal, which accounts for nearly 80% of the total PCA in the western Yellow Sea, increased from  $50 \text{ km}^2$  in 2000 to  $240 \text{ km}^2$  in 2015. According to satellite observations, the mode-I *P. yezoensis* cultivation never led to floating *Ulva* MABs. In the contrary, the *Ulva* MABs originated from the mode-II cultivation region of the Jiangsu Shoal would reach the mode-I region under favorable wind condition, for instance, in the summer of 2016 (Xing et al., 2018).

In the mode-II cultivation region of the Jiangsu Shoal, i.e., the origin of the *Ulva* green tide (Liu et al., 2009; Wang et al., 2015; Xing et al., 2018), the PCA increased from  $125 \text{ km}^2$  in 2006 to  $160 \text{ km}^2$  in 2007,

and to  $170 \text{ km}^2$  in 2008, with an increase rate of no  $> 20\%$  per year. Therefore, similar to the increase of the mode-I PCA near Lianyungang, which is not related to the occurrence of green tide, the expansion rate of the total PCA in the Jiangsu Shoal did not account for the sudden occurrence of large-scale green tides in 2007 and 2008 (Liu et al., 2009; Hu et al., 2010; Xing et al., 2015b). Thus, the green macroalgae causing green tide must have come from distinct locations of the Jiangsu Shoal, which are shown in the following subsections.

#### 3.2. Evolution of *P. yezoensis* cultivation in the Jiangsu shoal and its impacts on green tide

Fig. 6 shows detailed spatio-temporal changes in mode-II *P. yezoensis* cultivation region of the Jiangsu Shoal. The time series of the maps show that the *P. yezoensis* cultivation in the Jiangsu Shoal expanded by about 100 km from the south to the north from 2000 to 2018. As shown in Fig. 6a, the *P. yezoensis* cultivation region from the north to the south of the Jiangsu Shoal is artificially segmented into six zones according to latitude, and the annual PCA in each sub-zone is then calculated. Fig. 6b shows that the PCA of the north part of the Jiangsu Shoal (zones Z1, Z2 and Z3) started to increase rapidly in 2006, especially in zones Z1 and Z2; the PCA in 2007 was about  $35 \text{ km}^2$  with a sharp increase by  $> 150\%$  from 2006, which was consistent with the first appearance of large-scale green tide in the summer of 2007 (Hu et al., 2010; Xing et al., 2011).

Note that the farming zones Z1, Z2 and Z3 were located in the

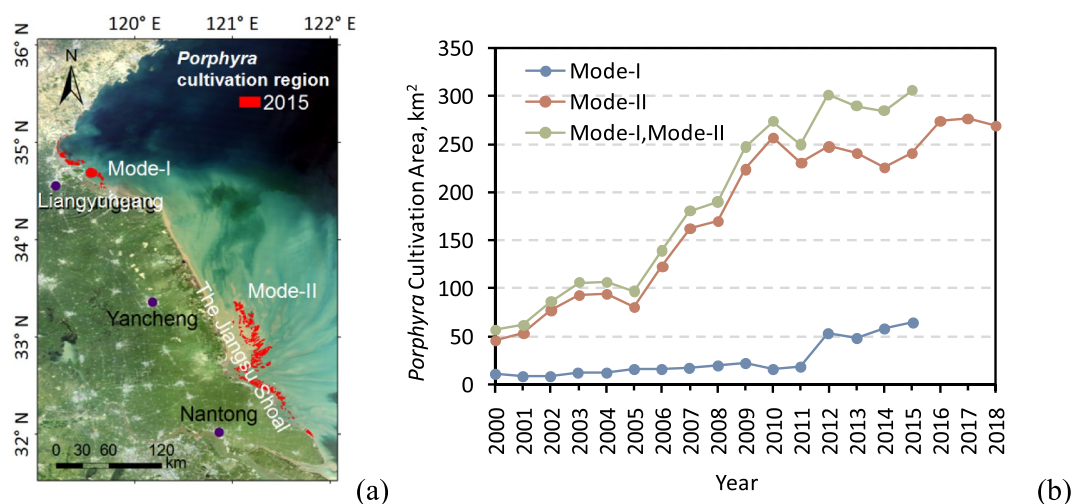


**Fig. 5.** (a) *P. yezoensis* cultivation regions (in red) in 2015 in the western Yellow Sea, and (b) *P. yezoensis* cultivation area (PCA) in 2000–2017: the mode-I PCA of Liangyungang (2000–2015), and the mode-II PCA of the Jiangsu Shoal (2000–2018). (For interpretation of the references to colour in this figure legend, the reader is referred to the web version of this article.)

offshore tidal flats about 30–60 km away from the coastal line; the cost of transportation of farming facilities in these zones was relatively higher. Workers were more likely to remove *Ulva* macroalgae from the facilities in situ to reduce the weight rather than collect them, thus increasing the chance of releasing *Ulva* macroalgae into sea water.

Fig. 7a and b show the historical magnitude of green tide in the

Yellow Sea by using the index of annual MD-MABs. In general, there was an increase trend in the MD-MABs ( $R^2 = 0.40$ ), especially in the period before 2017 ( $R^2 = 0.54$ ), which is also in agreement with the interannual change in yearly biomass and coverage of green macroalgae estimated in other studies (Qi et al., 2016; Hu et al., 2017). Even excluding from the time series the two years of 2015 and 2016 with the

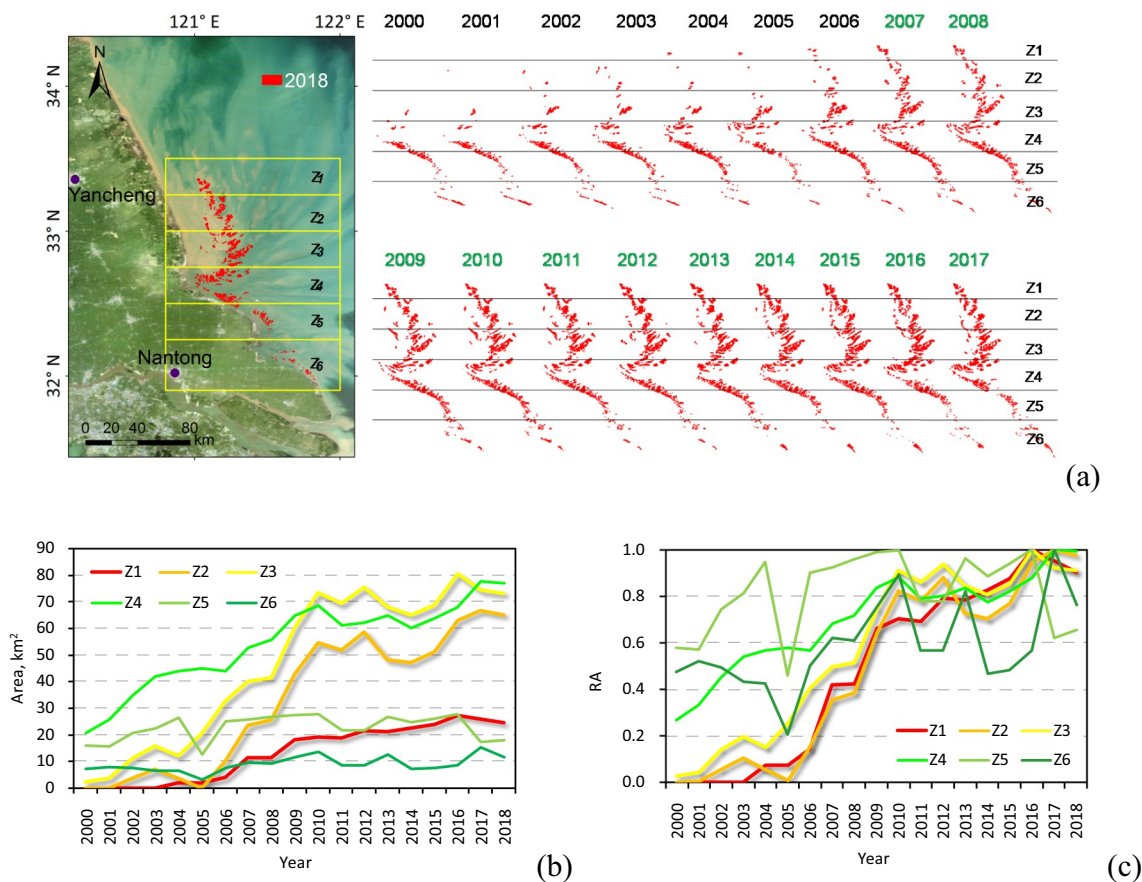


**Fig. 6.** (a) Annual distributions of *P. yezoensis* cultivation (patches in red) in the Jiangsu Shoal (2000–2018). Six zones marked by Z1, Z2, ..., Z6 are from the north to the south of the cultivation region, (b) the absolute area of the PCAs of six sub-zones, and (c) the relative area (RA), i.e., the ratio of yearly absolute area to its maximum value in the same zone in the period of 2000–2018. (For interpretation of the references to colour in this figure legend, the reader is referred to the web version of this article.)

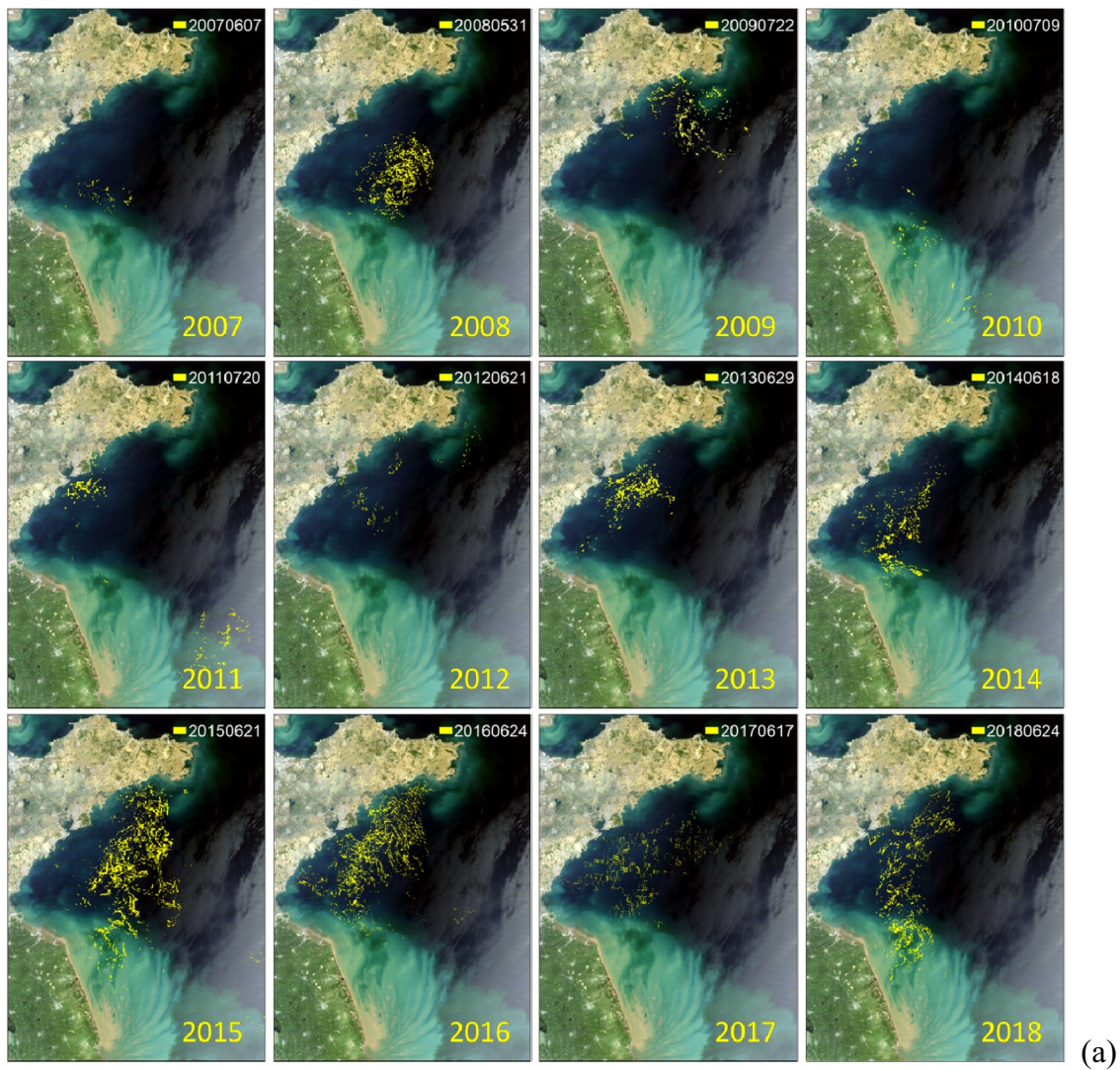


Fig. 7. (a) Spatial distributions (yellow patches) of the annual maximum daily macroalgal blooms (MD-MABs) with the dates (YYYYMMDD), and (b) corresponding covering areas (km<sup>2</sup>) in the Yellow Sea during the period from 2007 to 2018. (For interpretation of the references to colour in this figure legend, the reader is referred to the web version of this article.)

largest MD-MABs, the increasing trend is still evident ( $R^2 = 0.49$ ). As seen in Fig. 8, the annual MD-MABs tend to be more correlated to the PCA in the north part of the Jiangsu Shoal cultivation region than in the other zones, e.g., the correlation coefficient between the MD-MABs and the PCA of zone Z1 is the largest ( $r = 0.63$ ). These results suggest that the occurrence of green tide is more likely correlated to the *P. yezoensis*

cultivation activities in the north part of the Jiangsu Shoal.

### 3.3. Drifting paths of early floating macroalgae from different source sites

The LPT model is used to simulate the drifting path of floating green macroalgae (*Ulva*) from the Jiangsu Shoal *P. yezoensis* cultivation region

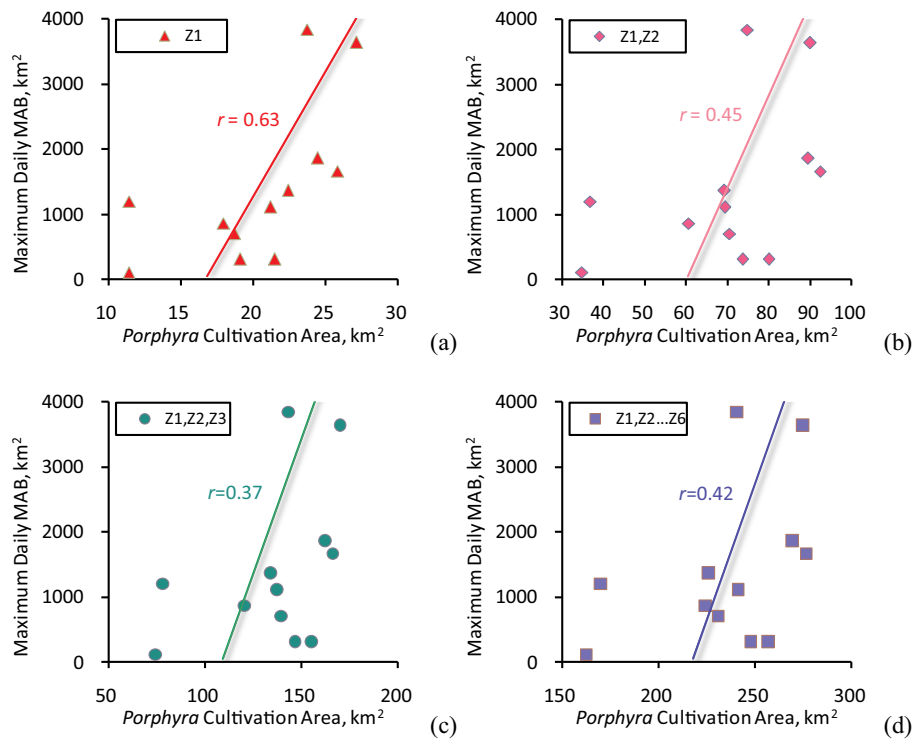


**Fig. 8.** Correlations between MD-MABs and *P. yezoensis* cultivation area of different zones: (a) Z1; (b) Z1 and Z2; (c) Z1, Z2 and Z3; and (d) the entire region of Z1, Z2, ..., Z6.

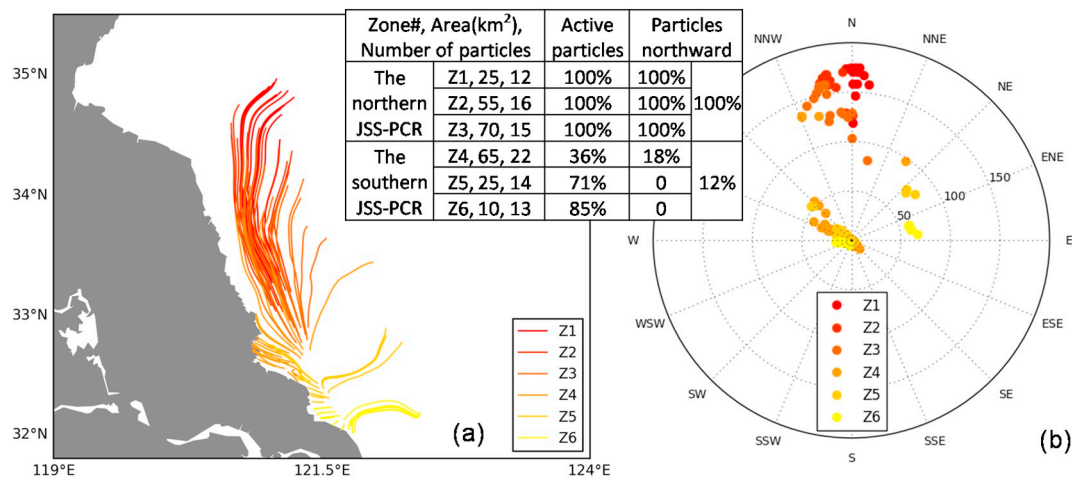


**Fig. 9.** (a) Trajectories of *Ulva* macroalgae particles released from the *P. yezoensis* cultivation region of Jiangsu Shoal (the JSS-PCR) from 15 April to 25 May; (b) Locations of all particles on May 25 relative to initial locations on April 15 of zones Z1, Z2, ... and Z6, respectively. The inset table shows the percentage of active particles and particles moving northward (NNW, N, NNE) till May 25 from the JSS-PCR where the area (km<sup>2</sup>) refers to the averaged annual *P. yezoensis* cultivation area in each zone during the period from 2016 to 2018 (for details, please refer to Fig. 6).

(JSS-PCR) from 15 April to 25 May. The release date of macroalgae particles in the LPT model is April 15 when the *P. yezoensis* cultivation facilities are recycled and green macroalgae are scraped from the facilities and discarded into sea water. The initial locations of *Ulva* macroalgae are randomly generated in the six zones (Z1-Z6) of the JSS-PCR. Fig. 9a shows the trajectories of *Ulva* particles originating from different zones of the JSS-PCR. Generally, *Ulva* macroalgae originating from the north part of the JSS-PCR (i.e., Z1, Z2 and Z3 shown in Fig. 6) tend to drift in a northward direction (Fig. 9a and b); and these *Ulva* macroalgae particles can drift to 35°N, about 150 km away from their origins on 25 May. These sites of macroalgae particles simulated by the LPT model are in good agreement with the actual sites observed by satellites (Xing et al., 2018; also see Fig. 10).

During the period from 15 April to 25 May, floating macroalgae particles may move across the boundary of the coastline, and become inactive due to beaching. As shown in Fig. 9, all the particles from the northern JSS-PCR (Z1, Z2 and Z3) are active, and move northward. Meanwhile, in the southern JSS-PCR (Z4, Z5 and Z6), the major part of macroalgae particles is active; however, no > 12% moves northward. And, a part of these particles may move eastward and southward, reaching the coastal waters of the Korean Peninsula in the Yellow Sea (Xing et al., 2011; Son et al., 2015; Xing and Hu, 2016) and of the Yangtze River Estuary in the East China Sea (Zhang et al., 2015a), respectively. The JSS-PCR is located in a radial sand ridge system and connected the open Yellow Sea through several tidal channels. The radial sand ridges indicate the dominating direction of tidal currents



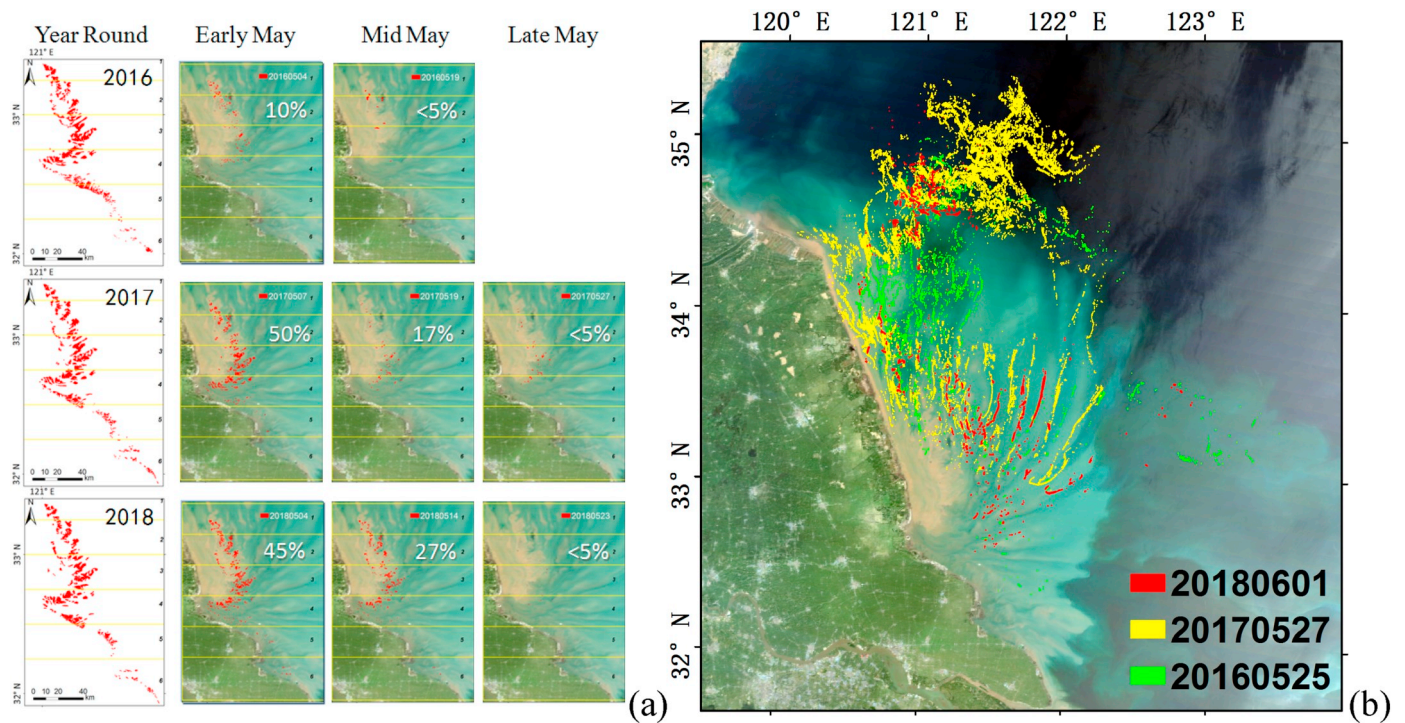


**Fig. 10.** (a) Distribution of *P. yezoensis* facilities (red patches) in Jiangsu Shoal in May. The percentage denotes the ratio of the temporal area to the year-round total area; and the *P. yezoensis*-facility recycling is assumed to be completed when it is < 5%. (b) Distributions of early *Ulva* MABs in 2016, 2017 and 2018 with the dates (YYYYMMDD), respectively. (For interpretation of the references to colour in this figure legend, the reader is referred to the web version of this article.)

(Wang et al., 2011; Zhong et al., 2018), and also show the major drifting channels of initial macroalgae particles from the JSS-PCR.

These simulation results suggest that floating macroalgae originated from the northern JSS-PCR contribute mostly to the massive green tide in the Yellow Sea, and give reasons to why the MD-MABs are more correlated to the expansion of *P. yezoensis* cultivation in the northern JSS-PCR.

The above satellite observations and LPT modeling results suggest that the northern JSS-PCR is the major source of *Ulva* blooms in the Yellow Sea. Thus, changes in the timing of the facility recycling and the corresponding release of *U. prolifera* macroalgae from the northern JSS-PCA may alter the magnitude of *Ulva* blooms effectively.

### 3.4. Effects of the timing of seaweed-facility recycling

Fig. 10a shows the distributions of *P. yezoensis* facilities in May of 2016, 2017 and 2018, indicating the timing of the *P. yezoensis*-facility recycling in the JSS-PCR. In the three years, the year-round total PCA had low interannual variation by no > 5%, while the timing of recycling facilities varied. In 2016, the *P. yezoensis*-facility recycling was completed in mid-May, while in 2017 and 2018, the completion of recycling was postponed to late May. The postponed recycling of *P. yezoensis* facilities in 2017 and 2018 was expected to postpone the release of green macroalgae removed from the facilities into the sea water; accordingly, the developing processes of early floating MABs would be altered.

Fig. 10b and Table 2 show the distributions and the coverage areas of early MABs in the same period of 2016, 2017 and 2018, respectively. On 25 May 2016, the coverage area of MABs was as much as 158 km<sup>2</sup>, while the estimated area of floating macroalgae were only 46% and 18% on the same days of 2017 and 2018 compared to that in 2016. On 14 May 2018, there was about 27% of the *P. yezoensis* facilities remained on the tidal flats, mainly in the northern JSS-PCR, while on 23 May 2018, *P. yezoensis* facilities left on the tidal flats were no > 5% of the total (Fig. 10a). The coverage area of floating macroalgae detected

**Table 2**

Covered areas of early *Ulva* blooms in 2016, 2017 and 2018. The numbers without underlines are satellite-derived covered areas. The underlined numbers are extrapolated based on a uniform growth rate and the satellite observation results on other dates; both the extrapolated values and their corresponding basis values are denoted by the same superscript symbols, respectively. The uniform growth rate of early floating *U. prolifera* macroalgae in the Jiangsu Shoal waters is assumed to be 20% per day (please refer to Section 2.4 for details).

Year	Covering area of early <i>U. prolifera</i> blooms, km <sup>2</sup>				
	23-May	25-May	27-May	1-June	3-June
2016	–	158	–	–	–
2017	–	<u>73</u> <sup>*</sup>	105 <sup>*</sup>	–	–
2018	<u>19.2</u> <sup>#</sup>	<u>27.6</u> <sup>#</sup>	–	99 <sup>#</sup>	<u>142</u> <sup>#</sup>
	5.7	–	–	–	137

by satellite was only 5.7 km<sup>2</sup> on 23 May 2018, less than one third of the value of 19.2 km<sup>2</sup> calculated on the basis of the satellite-derived result of 99 km<sup>2</sup> on 1 June 2018. This difference is mainly due to the fact that a part of small early floating macroalgae patches were not seen on the satellite image on 23 May 2018. While on 3 June 2018, the satellite-derived area was 137 km<sup>2</sup>, very close to the estimated area of 142 km<sup>2</sup> (the relative difference is 3.6%), which suggests that the MABs on 1 June 2018 were large enough for satellite detection and the empirical growth rate of 20% in Eq. (2) is reasonable for the early MABs.

The above observations in 2016, 2017 and 2018 show that the postponed *P. yezoensis*-facility recycling in May tended to reduce the magnitude of early MABs. Accordingly, as shown in Fig. 7, the MD-MABs in 2016 were about two times of those in 2017 and 2018, which is generally consistent with the early MABs in those three years. Over a longer period from 2013 to 2018, the MD-MABs of 2015 and 2016 were the largest ones, about two times of those in 2013, 2014, 2017, and 2018 (Fig. 7), while the remaining *P. yezoensis* facility areas in early May of 2015 and 2016 were no more than one half of those in the other

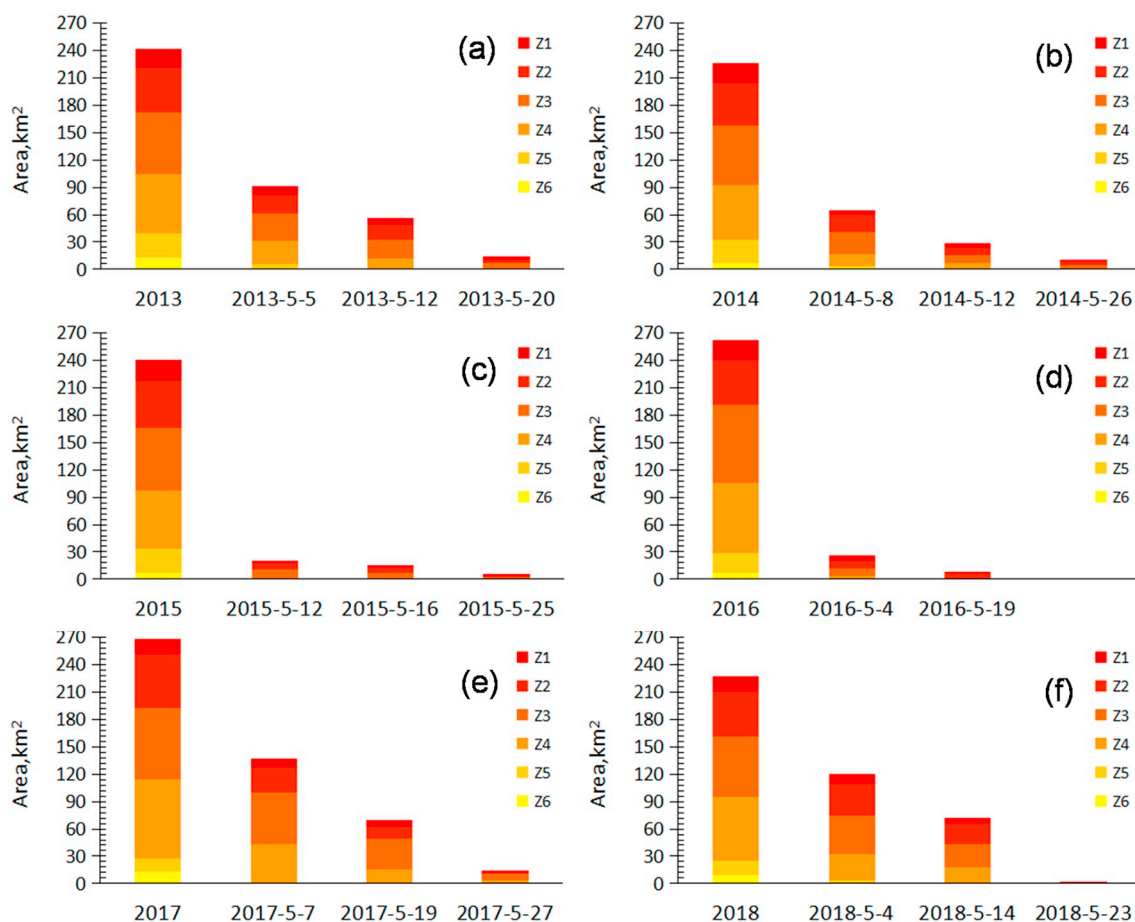


Fig. 11. Annual areas (km<sup>2</sup>) of *P. yezoensis* farming region and the remaining facilities on different dates in May (year-month-day): (a) 2013, (b) 2014, (c) 2015, (d) 2016, (e) 2017 and (f) 2018. The setting of zone Z1, Z2, Z3, Z4, Z5 and Z6 is the same as that in Fig. 6.

years (Fig. 11). These results suggest that the postponed *P. yezoensis*-facility recycling, while postponing early MABs, may also be considered as the main factor responsible for a reduced annual biomass of MABs.

### 3.5. Discussion on the growth rates of attached and floating green macroalgae

The recycling of *P. yezoensis* farming facilities in April and May (as shown in Fig. 4) is the key process leading to the release of attached green macroalgae into sea water. The observed reductions in both the early floating MABs and the annual MD-MABs connected to the postponed release of attached macroalgae from the facilities into sea water, imply a lower growth rate for green macroalgae attached to the facilities compared to that of floating green macroalgae in sea water.

In-situ experiments (Zhang et al., 2013) and satellite observations (Xing et al., 2018) showed that the growth rate of floating green macroalgae in May in the Jiangsu Shoal waters was usually higher than 20% per day. According to the results of in-situ observations on the biomass of green macroalgae attached to the facilities at the Jiangsu Shoal (Fan et al., 2015; Wang et al., 2015; Zhang et al., 2015b), the growth rates of green macroalgae attached to the facilities in April and May were no > 12.5% per day (Zhang et al., 2015b), which is much lower than the growth rate of green macroalgae in floating mode in the same season.

Actually, as shown by the in-situ photos in Figs. 1, 2 and 4, the *P. yezoensis* nets were intentionally placed to be above water to ensure certain exposure duration in air, which is one common and traditional practice in *P. yezoensis* farming, the so called “sun exposure” (Wang, 1992). One of the important purposes of “sun exposure” is to prevent

the reproduction of fouling green macroalgae dominated by *U. prolifera*. The acute stress of exposure and emersion can reduce the growth of green macroalgae (Sampath-Wiley et al., 2008). In comparison with the unlimited space of sea water for the growth of floating macroalgae, the biomass of macroalgae attached to farming facilities should be constrained by its substrate space.

In addition to the source biomass of *U. prolifera* on the *P. yezoensis* facilities, other factors also modulate the magnitude of the green tide, e.g., light radiation, water temperature and nutrient supply (Xing et al., 2015b; Jin et al., 2018), which all have spatio-temporal variation. Floating green macroalgae in late May and June may face less favorable conditions for growth. Xing et al. (2018) reported that *Ulva* green tide had lower growth rate (no > 10% per day) after June when the green tide drifted out of the eutrophicated turbid plume of the Jiangsu Shoal (Fig. 10b). Thus, the postponed release of green macroalgae into sea water reduced the fast-growing period and the annual biomass (the MD-MABs).

In general, the postponed release of green macroalgae into sea water during the seaweed-facility recycling in April and May can reduce the biomass of *U. prolifera* green tide. This finding implies that the *Ulva* green tide can be controlled if suitable countermeasures are applied to change the *P. yezoensis* cultivation in the northern Jiangsu Shoal.

## 4. Conclusions and prospective

We present detailed spatio-temporal changes in *P. yezoensis* cultivation region (2000–2018) in the Jiangsu coastal waters, and the annual maximum daily macroalgal blooms which are dominated by *U. prolifera* in the Yellow Sea. The results of correlation analysis and

numerical simulation indicate that the expanding *P. yezoensis* cultivation in the tidal flats of the northern Jiangsu Shoal is the main reason for the occurrence of large-scale *Ulva* macroalgae blooms every summer in the Yellow Sea since 2007. The postponed recycling of the *P. yezoensis* facilities in April and May, in postponing the occurrence of early *Ulva* macroalgae blooms, reduced the magnitude of the annual biomass, which verifies that green tide is manageable at the source location.

These findings indicate that not all the *P. yezoensis* cultivation in the Yellow Sea contributed to floating macroalgae blooms, and that the spatio-temporal control of marine aquaculture is critical for the associated hazard management and coastal ocean sustainability. Three aspects should be considered for managing the green tide in the Yellow Sea:

- (1) Using multi-sensor, multi-scale and multi-temporal observations to monitor the dynamics in the *P. yezoensis* farming and the facility recycling in the northern Jiangsu Shoal as the early warning of green tide and for further early countermeasures, e.g., macroalgae-collecting campaigns.
- (2) Optimizing the spatial planning of the *P. yezoensis* cultivation, and translocating the *P. yezoensis* farming region on the tidal flat of the northern Jiangsu Shoal to other deeper places (Titlyanov and Titlyanova, 2010) and using the cultivation mode-II, e.g., in the Lianyungang cultivation region and the Shandong Peninsula coastal waters.
- (3) Applying good seaweed-aquaculture practices to collect green macroalgae as bio-resources. This is also applicable to the golden tide of *Sargassum* recently confirmed in the Yellow Sea and East China Sea (Xing and Hu, 2016; Xing et al., 2017; Qi et al., 2017), which were partly contributed by marine aquaculture in a similar way to the green tide, i.e., the *Sargassum horneri* originally attached to aquaculture facilities were disposed as biofouling and released into sea water.

## Acknowledgements

This work was supported by the National Natural Science Foundation of China (Nos. 41676171 and 4181101363), the Chinese Academy of Science Strategic Priority Research Programme (Nos. XDA19060203 and XDA19060501), the Qingdao National Laboratory for Marine Science and Technology of China (No. 2016ASKJ02), the China Agriculture Research System (CARS-50), and the ESA (EU) - MOST (China) Dragon 4 Programme (project ID 31451-6). The surface current velocity data are from the Marine Science Data Center of Chinese Academy of Sciences. GaoFen-1 images are from CRESDA, Sentinel-1 and -2 images are from ESA, Landsat images are from USGS, and MODIS images are from NASA. The authors are grateful for the encouragement and suggestions from three anonymous reviewers, which improved the manuscript greatly.

## References

Bao, M., Guan, W., Yang, Y., Cao, Z., Chen, Q., 2015. Drifting trajectories of green algae in the western Yellow Sea during the spring and summer of 2012. *Estuarine Coastal & Shelf Science* 163, 9–16.

Bohórquez, J., Papaspyrou, S., Yúfera, M., van Bergeijk, S.A., García-Robledo, E., 2013. Effects of green macroalgal blooms on the meiofauna community structure in the Bay of Cádiz. *Mar. Pollut. Bull.* 70 (1–2), 10–17.

Fan, S., Fu, M., Wang, Z., Zhang, X., Song, W., Li, Y., Liu, G., Shi, X., Wang, X., Zhu, M., 2015. Temporal variation of green macroalgal assemblage on *Porphyra* aquaculture rafts in the Subei Shoal, China. *Estuar. Coast. Shelf Sci.* 163, 23–28.

Hu, C., 2009. A novel ocean color index to detect floating algae in the global oceans. *Remote Sens. Environ.* 113, 2118–2129.

Hu, C., He, M., 2008. Origin and offshore extent of floating algae in Olympic sailing area. *Eos, Am. Geophys. Union Trans.* 89, 302–303.

Hu, C., Li, D., Chen, C., Ge, J., Muller-Karger, F. E., Liu, J., ... He, M.-X. (2010). On the recurrent *Ulva* prolifera blooms in the Yellow Sea and East China Sea. *J. Geophys. Res.*, 115, C05017. <https://doi.org/10.1029/2009JC005561>.

Hu, L., Hu, C., He, M.-X., 2017. Remote estimation of biomass of *Ulva prolifera* macroalgae in the Yellow Sea. *Remote Sens. Environ.* 192, 217–227.

Hu, L., Zeng, K., Hu, C., He, M.-X., 2019. On the remote estimation of *Ulva* prolifera areal coverage and biomass. *Remote Sens. Environ.* 223, 194–207.

Jin, S., Liu, Y., Sun, C., Wei, X., Li, H., Han, Z., 2018. A study of the environmental factors influencing the growth phases of *Ulva* prolifera in the southern Yellow Sea, China. *Mar. Pollut. Bull.* 135, 1016–1025.

Keesing, J.K., Liu, D., Fearn, P., Garcia, R., 2011. Inter- and intra-annual patterns of *Ulva* prolifera green tides in the Yellow Sea during 2007–2009, their origin and relationship to the expansion of coastal seaweed aquaculture in China. *Mar. Pollut. Bull.* 62, 1169–1182.

Lapointe, B.E., Barile, P.J., Yentsch, C.S., 2004. The physiology and ecology of macroalgal blooms (green tides) on coral reefs off northern Palm Beach County, Florida (USA). *Harmful Algae* 3, 185–268.

Lee, J.H., Pang, I.C., Moon, I.J., Ryu, J.H., 2011. On physical factors that controlled the massive green tide occurrence along the southern coast of the Shandong peninsula in 2008: a numerical study using a particle-tracking experiment. *J. Geophys. Res.* 116 (2011), C12036. <https://doi.org/10.1029/2011JC007512>.

Li, L., Xing, Q., Li, X., Yu, D., Zhang, J., Zou, J., 2018. Assessment of the impacts from the world's largest floating macroalgae blooms on the water clarity at the west Yellow Sea using MODIS data (2002–2016). *IEEE J. Sel. Top. Appl. Earth Obs. Remote Sens.* 11, 1397–1402.

Liu, D., Keesing, J.K., Xing, Q., Shi, P., 2009. World's largest macroalgal bloom caused by expansion of seaweed aquaculture in China. *Mar. Pollut. Bull.* 58 (6), 888–895.

Qi, L., Hu, C., Xing, Q., Shang, S., 2016. Long-term trend of *Ulva* prolifera blooms in the western Yellow Sea. *Harmful Algae* 58, 35–44.

Qi, L., Hu, C., Wang, M., Shang, S., Wilson, C., 2017. Floating algae blooms in the East China Sea. *Geophys. Res. Lett.* 44. <https://doi.org/10.1002/2017GL075525>.

Qiao, F., Wang, G., Lü, X., Diao, D., 2011. Drift characteristics of green macroalgae in the Yellow Sea in 2008 and 2010. *China Science Bulletin* 56, 2236–2242.

Sampath-Wiley, P., Neeffus, C.D., Jahnke, L.S., 2008. Seasonal effects of sun exposure and emersion on intertidal seaweed physiology: fluctuations in antioxidant contents, photosynthetic pigments and photosynthetic efficiency in the red alga *Porphyra umbilicalis* Kützinger (Rhodophyta, Bangiales). *J. Exp. Mar. Biol. Ecol.* 361, 83–91.

Shen, H., Perrie, W., Liu, Q., He, Y., 2014. Detection of macroalgae blooms by complex SAR imagery. *Mar. Pollut. Bull.* 78, 190–195.

Shi, W., Wang, M. (2009). Green macro-algae blooms in the Yellow Sea during the spring and summer of 2008. *J. Geophys. Res.*, 114, p. C12010, <https://doi.org/10.1029/2009JC005513>.

Son, Y.B., Choi, B.-J., Kim, Y.H., Park, Y.-G., 2015. Tracing floating green algae blooms in the Yellow Sea and the East China Sea using GOCI satellite data and Lagrangian transport simulations. *Remote Sens. Environ.* 156, 21–33.

Titlyanov, E.A., Titlyanova, T.V., 2010. Seaweed cultivation: methods and problems. *Russ. J. Mar. Biol.* 36 (4), 227–242.

Wang, H., 1992. Comprehensive approaches of preventing green macroalgae in seaweed culture. *J. Aquac.* 1, 5 (In Chinese).

Wang, X.H., Li, L., Bao, X., Zhao, L.D., 2009. Economic cost of an algae bloom cleanup in China's 2008 Olympic sailing venue. *Eos Transactions American Geophysical Union* 90 (28), 238–239.

Wang, X.H., Qiao, F., Lu, J., Gong, F., 2011. The turbidity maxima of the northern Jiangsu shoal-water in the Yellow Sea, China. *Estuar. Coast. Shelf Sci.* 93, 202–211.

Wang, Z., Xiao, J., Fan, S., Li, Y., Liu, X., Liu, D., 2015. Who made the world's largest green tide in China?—an integrated study on the initiation and early development of the green tide in Yellow Sea. *Limnology & Oceanography* 60 (4), 1105–1117.

Wang, W., Zhang, G., Sun, X., Zhang, F., Zhang, X. (2019). Temporal variability in zooplankton community in the western Yellow Sea and its possible links to green tides. *PeerJ* 7:e6641, <https://doi.org/https://doi.org/10.7717/peerj.6641>.

Warren, C., DuPont, J., Abdel-Moati, M., Hobeichi, S., Palandro, D., Purkis, S. 2015. Toward the development of a remote sensing and field data framework to aid management decisions in the state of Qatar coastal environment, Qatar University Life Science Symposium, <http://dx.doi.org/https://doi.org/10.5339/qproc.2015.qulss2015.13>.

Wei, Z., Xing, Q., Guo, R., Li, L., 2018. Study on the spatial distribution variation of *Porphyra yezoensis* aquaculture in the southern Yellow Sea during the period 2000–2015 retrieved by satellite remote sensing. *Journal of Ocean Technology* 2018 (4). <https://doi.org/10.3969/j.issn.1003-2029.2018.04.002>.

Xing, Q., Hu, C., 2016. Mapping macroalgal blooms in the Yellow Sea and East China Sea using HJ-1 and Landsat data: application of a virtual baseline reflectance height technique. *Remote Sens. Environ.* 178, 113–126.

Xing, Q., Loisel, H., Schmitt, F., Shi, P., Liu, D., Keesing, J., 2009. Detection of the green tide at the Yellow Sea and tracking its wind-forced drifting by remote sensing. *Geophys. Res. Abstr.* 11 (EGU2009-577, EGU General Assembly 2009, Vienna).

Xing, Q., Zheng, X., Shi, P., Hao, J., Yu, D., Liang, S., ... Zhang, Y., 2011. Monitoring "GreenTide" in the Yellow Sea and the East China Sea using multi-temporal and multi-source remote sensing images. *Spectrosc. Spectr. Anal.* 31, 1644–1647 (in Chinese with English abstract).

Xing, Q., Hu, C., Tang, D., Tian, L., Tang, S., Wang, X.H., Lou, M., Gao, X., 2015a. World's largest macroalgal blooms altered phytoplankton biomass in summer in the Yellow Sea: satellite observations. *Remote Sens.* 7 (9), 12297–12313.

Xing, Q., Tosi, L., Braga, F., Gao, X., Gao, M., 2015b. Interpreting the progressive eutrophication behind the world's largest macroalgal blooms with water quality and ocean color data. *Nat. Hazards* 78 (1), 7–21.

Xing, Q., Guo, R., Wu, L., Cong, M., An, D., Qin, S., Li, X., 2017. High-resolution satellite observations of a new hazard of "Golden Tides" caused by floating *Sargassum* in winter in the Yellow Sea. *IEEE Geosci. Remote Sens. Lett.* 14 (10), 1815–1819.

Xing, Q., Wu, L., Tian, L., Cui, T., Li, L., Gao, X., Wu, M., 2018. Remote sensing of early-stage green tide in the Yellow Sea for floating-macroalgae collecting campaign. *Mar. Pollut. Bull.* 133, 150–156.

- Xu, Q., Zhang, H., Cheng, Y., Zhang, S., Zhang, W., 2016. Monitoring and tracking the green tide in the Yellow Sea with satellite imagery and trajectory model. *IEEE Journal of Selected Topics in Applied Earth Observations and Remote Sensing*. <https://doi.org/10.1109/JSTARS.2016.2580000>.
- Yang, D., Huang, R., Yin, B., Feng, X., Chen, H., Qi, J., Benthuyens, J.A., 2018. Topographic beta spiral and onshore intrusion of the Kuroshio Current. *Geophys. Res. Lett.* 45, 287–296. <https://doi.org/10.1002/2017GL076614>.
- Zhang, J., Huo, Y., Yu, K., Chen, Q., He, Q., Han, W., Chen, L., Cao, J., Shi, D., He, P., 2013. Growth characteristics and reproductive capability of green tide algae in Rudong coast, China. *J. Appl. Phycol.* 25, 795–803.
- Zhang, J.H., Liu, C.C., Yang, L.L., Gao, S., Ji, X., Huo, Y.Z., Yu, K.F., Xu, R., He, P.M., 2015a. The source of the *Ulva prolifera* blooms in the East China Sea by the combination of morphological, molecular and numerical analysis. *Estuar. Coast. Shelf Sci.* 164, 418–424.
- Zhang, Q., Liu, Q., Yu, R., Kang, Z.-Y., Guo, W., Ding, Y.-M., Chen, J.-H., Wang, Y.-F., Li, Y., Yan, T., Zhou, M.-J., 2015b. Application of a fluorescence in situ hybridization (FISH) method to study green tides in the Yellow Sea. *Estuar. Coast. Shelf Sci.* 163, 112–119.
- Zhang, J., Zhao, P., Huo, Y., Yu, K., He, P., 2017. The fast expansion of *Pyropia aquaculture* in “Sansha” regions should be mainly responsible for the *Ulva prolifera* blooms in Yellow Sea. *Estuar. Coast. Shelf Sci.* 189, 58–65.
- Zheng, X., Xing, Q., Li, L., Shi, P., 2011. Numerical simulation of the 2008 green tide in the Yellow Sea, marine. *Science* 35 (7), 82–87.
- Zhong, Y.-Z., Li, Y., Wu, X.-B., Gao, S., Zhou, T., Wang, Y.P., Gao, J.-H., 2018. Morphodynamics of a tidal ridge system in the southwestern Yellow Sea: HF radar study. *Estuar. Coast. Shelf Sci.* 206, 27–37.
- Zhou, Y.P., Tan, L.J., Pang, Q.T., Li, F., Wang, J.T., 2015. Influence of nutrients pollution on the growth and organic matter output of *Ulva prolifera* in the southern Yellow Sea, China. *Mar. Pollut. Bull.* 95 (1), 107–114.